5.1 The ferromagnetic hcp-crystal

In Chapter 3, we considered the linear response of a system of magnetic moments placed on a Bravais lattice and coupled by the Heisenberg interaction. We shall now generalize this treatment to the hexagonal close-packed crystal structure of the heavy rare earth metals, in which there is a basis of two ions per unit cell, constituting two identical sublattices which, for convenience, we number 1 and 2. The surroundings of the atoms belonging to each of the two sublattices are identical, except for an inversion. Introducing the following Fourier transforms:

$$\mathcal{J}_{ss'}(\mathbf{q}) = \sum_{j \in s'-subl.} \mathcal{J}(ij)\, e^{-i\mathbf{q}\cdot(\mathbf{R}_i - \mathbf{R}_j)} \qquad ; \quad i \in s\text{-sublattice}, \tag{5.1.1a}$$

we have, for an hcp crystal,

$$\begin{aligned} &\mathcal{J}_1(\mathbf{q}) \equiv \mathcal{J}_{11}(\mathbf{q}) = \mathcal{J}_{22}(\mathbf{q}) \\ &\mathcal{J}_2(\mathbf{q}) \equiv \mathcal{J}_{12}(\mathbf{q}) = \mathcal{J}_{21}(-\mathbf{q}) = \mathcal{J}_{21}^*(\mathbf{q}), \end{aligned} \tag{5.1.1b}$$

where $\mathcal{J}_1(\mathbf{q})$ is real. Defining the four Fourier transforms $\overline{\overline{\chi}}_{ss'}(\mathbf{q}, \omega)$ of the susceptibility tensor equivalently to (5.1.1a), we obtain from the

RPA equation (3.5.7):

$$\begin{aligned}\overline{\overline{\chi}}_{11}(\mathbf{q},\omega) &= \overline{\overline{\chi}}^{o}(\omega)\left\{1+\mathcal{J}_{11}(\mathbf{q})\,\overline{\overline{\chi}}_{11}(\mathbf{q},\omega)+\mathcal{J}_{12}(\mathbf{q})\,\overline{\overline{\chi}}_{21}(\mathbf{q},\omega)\right\}\\ \overline{\overline{\chi}}_{21}(\mathbf{q},\omega) &= \overline{\overline{\chi}}^{o}(\omega)\left\{\mathcal{J}_{21}(\mathbf{q})\,\overline{\overline{\chi}}_{11}(\mathbf{q},\omega)+\mathcal{J}_{22}(\mathbf{q})\,\overline{\overline{\chi}}_{21}(\mathbf{q},\omega)\right\},\end{aligned} \tag{5.1.2}$$

assuming that the MF susceptibility $\overline{\overline{\chi}}^{o}(\omega)$ is the same for all the sites, as in a paramagnet or a ferromagnet. These matrix equations may be solved straightforwardly, and using (5.1.1*b*) we find

$$\begin{aligned}\overline{\overline{\chi}}_{11}(\mathbf{q},\omega) &= \overline{\overline{D}}(\mathbf{q},\omega)^{-1}\{1-\overline{\overline{\chi}}^{o}(\omega)\,\mathcal{J}_1(\mathbf{q})\}\,\overline{\overline{\chi}}^{o}(\omega)\\ \overline{\overline{\chi}}_{21}(\mathbf{q},\omega) &= \overline{\overline{D}}(\mathbf{q},\omega)^{-1}\left\{\overline{\overline{\chi}}^{o}(\omega)\right\}^{2}\mathcal{J}_2(-\mathbf{q}),\end{aligned} \tag{5.1.3a}$$

where

$$\begin{aligned}\overline{\overline{D}}(\mathbf{q},\omega) &= \left\{1-\overline{\overline{\chi}}^{o}(\omega)\,\mathcal{J}_1(\mathbf{q})\right\}^{2}-\left\{\overline{\overline{\chi}}^{o}(\omega)\,|\mathcal{J}_2(\mathbf{q})|\right\}^{2}\\ &= \left(1-\overline{\overline{\chi}}^{o}(\omega)\left\{\mathcal{J}_1(\mathbf{q})+|\mathcal{J}_2(\mathbf{q})|\right\}\right)\left(1-\overline{\overline{\chi}}^{o}(\omega)\left\{\mathcal{J}_1(\mathbf{q})-|\mathcal{J}_2(\mathbf{q})|\right\}\right),\end{aligned} \tag{5.1.3b}$$

and, by symmetry,

$$\overline{\overline{\chi}}_{22}(\mathbf{q},\omega)=\overline{\overline{\chi}}_{11}(\mathbf{q},\omega) \qquad \text{and} \quad \overline{\overline{\chi}}_{12}(\mathbf{q},\omega)=\overline{\overline{\chi}}_{21}(-\mathbf{q},\omega). \tag{5.1.3c}$$

If $\overline{\overline{\chi}}^{o}(\omega)$ contains only one pole, as in the case of the Heisenberg ferromagnet, then $\overline{\overline{D}}(\mathbf{q},\omega)^{-1}$ in (5.1.3*a*) generates two poles, corresponding to the existence of both an *acoustic* and an *optical* mode at each $\mathbf{q}$-vector. $\mathcal{J}_2(\mathbf{0})$ must be real and, since it is also positive in a ferromagnet, the acoustic mode arises from the zero of the first factor in (5.1.3*b*), its energy therefore being determined by the effective coupling parameter $\mathcal{J}_1(\mathbf{q})+|\mathcal{J}_2(\mathbf{q})|$. On the other hand, if $\mathcal{J}_2(\mathbf{0})$ is negative, as it is in paramagnetic Pr, it is the second factor which gives the acoustic mode. The nomenclature results from the circumstance that the deviations of the moments from their equilibrium values are in phase in the acoustic mode in the limit of $\mathbf{q}\to\mathbf{0}$, and it therefore dominates the neutron cross-section. The inelastic neutron scattering is determined by (4.2.2) and (4.2.3), i.e. by

$$\begin{aligned}\overline{\overline{\chi}}(\boldsymbol{\kappa},\omega) &= \frac{1}{N}\sum_{ij}\overline{\overline{\chi}}(ij,\omega)\,e^{-i\boldsymbol{\kappa}\cdot(\mathbf{R}_i-\mathbf{R}_j)}=\frac{1}{2}\sum_{ss'}\overline{\overline{\chi}}_{ss'}(\boldsymbol{\kappa},\omega)\\ &= \overline{\overline{D}}(\boldsymbol{\kappa},\omega)^{-1}\Big\{1-\overline{\overline{\chi}}^{o}(\omega)\big(\mathcal{J}_1(\boldsymbol{\kappa})-\tfrac{1}{2}[\mathcal{J}_2(\boldsymbol{\kappa})+\mathcal{J}_2(-\boldsymbol{\kappa})]\big)\Big\}\,\overline{\overline{\chi}}^{o}(\omega),\end{aligned} \tag{5.1.4}$$

where $N=2N_0$ is the number of atoms. Introducing $\boldsymbol{\kappa}=\mathbf{q}+\boldsymbol{\tau}$, with $\mathbf{q}$ lying in the primitive zone, we may write this result as a sum of the acoustic and optical response functions:

$$\begin{aligned}\overline{\overline{\chi}}_{\mathrm{Ac}}(\mathbf{q},\omega) &= \left\{1-\overline{\overline{\chi}}^{o}(\omega)(\mathcal{J}_1(\mathbf{q})+\nu|\mathcal{J}_2(\mathbf{q})|)\right\}^{-1}\overline{\overline{\chi}}^{o}(\omega)\\ \overline{\overline{\chi}}_{\mathrm{Op}}(\mathbf{q},\omega) &= \left\{1-\overline{\overline{\chi}}^{o}(\omega)(\mathcal{J}_1(\mathbf{q})-\nu|\mathcal{J}_2(\mathbf{q})|)\right\}^{-1}\overline{\overline{\chi}}^{o}(\omega),\end{aligned} \tag{5.1.5}$$

where $\nu = \pm 1$ denotes the sign of $\mathcal{J}_2(\mathbf{0})$. $\mathcal{J}_1(\boldsymbol{\kappa}) = \mathcal{J}_1(\mathbf{q})$ is real, whereas

$$\mathcal{J}_2(\boldsymbol{\kappa}) = \mathcal{J}_2(\mathbf{q})\, e^{i\boldsymbol{\tau}\cdot\boldsymbol{\rho}} = \nu|\mathcal{J}_2(\mathbf{q})|e^{i\varphi}, \tag{5.1.6a}$$

defining the phase $\varphi = \varphi(\boldsymbol{\kappa})$, and $\boldsymbol{\rho} = \mathbf{d}_2 - \mathbf{d}_1$ is the vector joining the two sublattices. In terms of these quantities, the susceptibility (5.1.4) may be written

$$\overline{\overline{\chi}}(\mathbf{q}+\boldsymbol{\tau},\omega) = \tfrac{1}{2}(1+\cos\varphi)\,\overline{\overline{\chi}}_{\mathrm{Ac}}(\mathbf{q},\omega) + \tfrac{1}{2}(1-\cos\varphi)\,\overline{\overline{\chi}}_{\mathrm{Op}}(\mathbf{q},\omega). \tag{5.1.6b}$$

The phase φ vanishes in the limit $\mathbf{q} \to \mathbf{0}$ if $\boldsymbol{\tau} = \mathbf{0}$, and the scattering cross-section then only depends on the isolated pole in the acoustic response function, in accordance with our definition above. Introducing the following lattice vectors of the hexagonal lattice:

$$\mathbf{a}_1 = (a,0,0) \qquad \mathbf{a}_2 = \big(-\frac{a}{2}, \frac{\sqrt{3}a}{2}, 0\big) \qquad \mathbf{a}_3 = (0,0,c), \tag{5.1.7a}$$

we find the corresponding reciprocal lattice vectors:

$$\mathbf{b}_1 = \big(\frac{2\pi}{a}, \frac{2\pi}{\sqrt{3}a}, 0\big) \qquad \mathbf{b}_2 = \big(0, \frac{4\pi}{\sqrt{3}a}, 0\big) \qquad \mathbf{b}_3 = \big(0,0,\frac{2\pi}{c}\big). \tag{5.1.7b}$$

Since $\boldsymbol{\rho} = \big(\frac{a}{2}, \frac{a}{2\sqrt{3}}, \frac{c}{2}\big)$,

$$\boldsymbol{\tau}\cdot\boldsymbol{\rho} = \frac{4\pi}{3}h + \frac{2\pi}{3}k + \pi l \qquad \text{with} \quad \boldsymbol{\tau} = (hkl) = h\mathbf{b}_1 + k\mathbf{b}_2 + l\mathbf{b}_3. \tag{5.1.8}$$

If $\mathbf{q}$ is parallel to the c-axis, $\mathcal{J}_2(\mathbf{q})$ is real. The phase φ in (5.1.6) is then $\boldsymbol{\tau}\cdot\boldsymbol{\rho}$ and, if the Miller indices h and k are both zero, $\varphi = \boldsymbol{\tau}\cdot\boldsymbol{\rho} = l\pi$. In this case, with $\boldsymbol{\kappa}$ in the c-direction, the inelastic scattering detects only the acoustic or the optical excitations, depending on whether l is respectively even or odd, and no energy gap appears at the zone boundary, even though l changes, because $\mathcal{J}_2(\mathbf{b}_3/2) = 0$ by symmetry. We may therefore use a *double-zone representation*, in which the dispersion relation for the excitations is considered as comprising a single branch extending twice the distance to the Brillouin zone boundary, corresponding to an effective unit cell of height $c/2$. We shall generally use this representation when discussing excitations propagating in the c-direction.

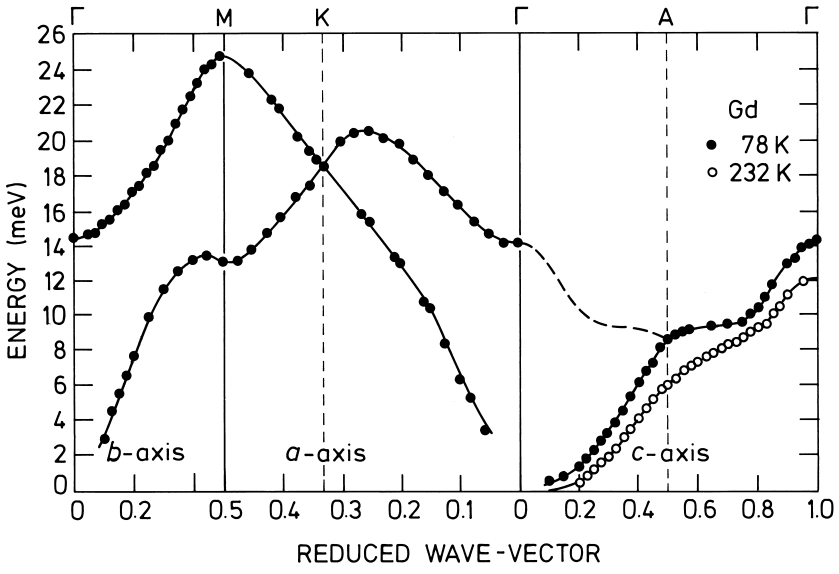

Fig. 5.1. Spin-wave dispersion relations for Gd, after Koehler *et al.* (1970). The two atoms of the hcp structure give rise to acoustic and optical branches. Since the single-ion anisotropy is negligible, the acoustic mode rises quadratically from the origin.

Because $L = 0$, so that $J = S$, anisotropy effects are small in Gd, and it is therefore a good approximation to a Heisenberg ferromagnet. Using the above procedure to generalize (3.5.26) to the hcp structure, we obtain the two branches of the excitation spectrum

$$\begin{aligned} E_{\mathbf{q}}^{\mathrm{Ac}} &= \langle J_z \rangle \big\{ \mathcal{J}_1(\mathbf{0}) + \mathcal{J}_2(\mathbf{0}) - \mathcal{J}_1(\mathbf{q}) - |\mathcal{J}_2(\mathbf{q})| \big\} \\ E_{\mathbf{q}}^{\mathrm{Op}} &= \langle J_z \rangle \big\{ \mathcal{J}_1(\mathbf{0}) + \mathcal{J}_2(\mathbf{0}) - \mathcal{J}_1(\mathbf{q}) + |\mathcal{J}_2(\mathbf{q})| \big\}, \end{aligned} \tag{5.1.9}$$

since $\mathcal{J}_2(\mathbf{0})$ is positive. The dispersion relations measured by inelastic neutron scattering by Koehler *et al.* (1970) are shown in Fig. 5.1. This figure illustrates the use of the double-zone representation when $\mathbf{q}$ is along the c-axis, resulting in a single spin-wave branch. The renormalization predicted by the simple RPA theory, that $E_{\mathbf{q}}(T)$ is proportional to σ, is not followed very precisely. σ changes from about 0.97 at 78 K to 0.66 at 232 K. As may be seen from Fig. 5.1, and from more extensive studies by Cable *et al.* (1985), the energies in the c-direction vary approximately like $\sigma^{0.5}$ at the largest wave-vectors, like σ in the middle of the branch, and faster than σ at small wave-vectors. However, it is also evident from the figure that the form of $\mathcal{J}(\mathbf{q})$ changes with decreasing magnetization, so some of the discrepancy between the simple

prediction and the observed behaviour at low temperatures may be due to changes of $\mathcal{J}(\mathbf{q})$. At higher temperatures, the RPA renormalization breaks down completely. The spin-wave energy at the zone boundary has only fallen by about a factor two at 292 K, very close to T_C. Furthermore, strongly-broadened neutron peaks are observed even at 320 K, well above the transition, close to the zone boundary in the basal plane, with energies of about $k_B T_C$. On the other hand, the low-energy spin waves progressively broaden out into diffusive peaks as T_C is approached from below.